



Published in final edited form as:

Chem Commun (Camb). 2012 September 18; 48(72): 9044–9046. doi:10.1039/c2cc34695h.

Photodynamic activity of viral nanoparticles conjugated with C₆₀

Amy M. Wen^a, Mary J. Ryan^{a,d}, Alice C. Yang^a, Kurt Breitenkamp^e, Jonathan K. Pokorski^f, and Nicole F. Steinmetz^{a,b,c}

Nicole F. Steinmetz: nicole.steinmetz@case.edu

^aDepartment of Biomedical Engineering, Case Western Reserve University, 10900 Euclid Avenue, Cleveland, OH 44106, USA, Tel: +1 216 368 5590

^bDepartment of Radiology, Case Western Reserve University, 10900 Euclid Avenue, Cleveland, OH 44106, USA, Tel: +1 216 368 5590

^cDepartment of Materials Science and Engineering, Case Western Reserve University, 10900 Euclid Avenue, Cleveland, OH 44106, USA, Tel: +1 216 368 5590

^dDepartment of Chemical and Materials Engineering, School of Engineering, University of Dayton, Dayton, OH 45469

^eDepartment of Chemistry, The Scripps Research Institute, 10550 North Torrey Pines Road, La Jolla, CA 92037

^fDepartment of Macromolecular Sciences and Engineering, Case Western Reserve University, 10900 Euclid Avenue, Cleveland, OH 44106, USA, Tel: +1 216 368 5590

Abstract

The development of viral nanoparticles (VNP) displaying multiple copies of the buckyball (C₆₀) and their photodynamic activity is described. VNP-C₆₀ conjugates were assembled using click chemistry. Cell uptake and cell killing using white light therapy and a prostate cancer cell line is demonstrated.

Photodynamic therapy (PDT) is a minimally invasive focal therapy, less invasive than surgery and resulting in fewer adverse effects compared to systemic chemotherapy.¹ In PDT, a photosensitizer is delivered systemically to the tumor and locally activated by a probe containing a low-power light source and optical fibers. Management of localized cancers using PDT holds great promise and is undergoing clinical tests. A wide array of photosensitizing drugs has been developed, such as porphyrins² and phthalocyanine dyes.³ Novel materials currently being explored include the buckyball (C₆₀) and its derivatives.⁴ Upon irradiation of C₆₀ with UV or white light, the molecule is excited to a triplet state, which can directly interact with oxygen to generate reactive singlet oxygen. The fullerene triplet can also be reduced by biological reductants to give the fullerene radical anion; electron transfer from the latter to oxygen generates the superoxide radical and ultimately produces highly reactive hydroxyl radicals through dissociation of hydrogen peroxide.⁵ Either event leads to cell death. C₆₀ is a highly hydrophobic material, and it has been reported that colloidal aggregates induce toxicity in human cells.⁶ A delivery vehicle is therefore required to further develop this material for *in vivo* PDT. Several approaches toward the solubilisation and stabilization of C₆₀ in aqueous media have been developed; these include C₆₀-micelle and liposome nanocomposites.⁷

Nevertheless, tissue-specific delivery of C₆₀-conjugates to cancerous cells *in vivo* remains challenging. Therefore we turned toward the development of a bio-inspired nanotechnology, specifically viral nanoparticles (VNPs) loaded with C₆₀ drug. Although the use of VNPs as carriers for the delivery of therapies is widely discussed, only two reports have been published describing the use of VNPs in PDT. Staphylococcus-targeted ruthenium-CCMV conjugates have been developed to treat bacterial infections,⁸ and MS2 particles loaded with porphyrins have been targeted to T-cells using receptor-specific aptamers as candidates for PDT in the treatment of leukemia.⁹ VNPs can be produced in large scale using molecular farming or fermentation. VNPs are highly multivalent and amendable through genetic engineering and chemical modification.¹⁰ Hundreds of copies of drugs, imaging moieties, or targeting ligands can be displayed on the exterior or interior VNP surfaces. We have previously shown that VNPs modified with targeting ligands can be effectively targeted to prostate tumors.¹¹ VNPs can be used as carriers for delivery of chemotherapies¹² and photosensitizers.¹³ In this study, we turned toward the development of bacteriophage Q β -C₆₀ conjugates as PDT agents for treatment of prostate cancer. The 30 nm-sized icosahedral capsid has $T = 3$ symmetry and is formed by 180 copies of a single coat protein. Q β displays 720 reactive Lys side chains, 4 each per 180 identical coat protein units.

Q β was modified with Oregon Green 488 (O488, Invitrogen) and C₆₀ at solvent-exposed surface lysines. *N*-hydroxysuccinimide (NHS) ester chemistry was used to conjugate O488 and an azide ligation handle (azido (PEO)₄ propionic acid succinimidyl ester, Invitrogen) to Q β (Scheme 1).

Copper-catalyzed azide-alkyne cycloaddition (CuAAC) was used to conjugate a propargyl-O-PEG-C₆₀ derivative¹⁴ (Scheme 1 and Supporting Information). The reaction was purified and analysed by size exclusion chromatography (SEC) (Fig. 1A). Fractions corresponding to labeled, intact particles (9–15 mL) were collected and concentrated with 10 kDa cut-off centrifugal filters. SEC indicated covalent attachment of C₆₀ and O488 to Q β particles (Fig. 1A). Native particles elute at 10.2 mL from the column, compared to 9.7 mL for Q β -C₆₀ and 10.1 mL for Q β -O488. The shift suggests that Q β -C₆₀ were larger in size; this is as expected, since C₆₀ measures approximately 1 nm in diameter. Attachment of O488 was validated based on the co-elution of O488 (Abs at 496 nm) with the Q β particles (Abs at 260 nm and 280 nm). O488 conjugation was determined using a Nanodrop spectrophotometer (Fig. 1B) and the characteristic extinction coefficient of O488 at 496 nm of 70,000 M⁻¹ cm⁻¹. Q β and Q β -C₆₀ were labeled with 110±10 dyes each. C₆₀ conjugation was monitored using native and denaturing SDS gel electrophoresis. After separation, the gels were photographed using Alphamager (Biosciences) imaging system after staining with Coomassie Blue (Fig. s 1C+D). In native gels, Q β particles change mobility based on charge and size. Mobility toward the anode increased upon azide conjugation; converting the amine group of Lys side chains into an azide results in decreased positive charge of the particles, thus enhancing the electrophoretic mobility toward the anode. Electrophoretic mobility is slowed down upon C₆₀-conjugation due to increased size of the complex; this is in good agreement with SEC data. In denaturing gels, heating of the sample and presence of the anionic detergent would likely separate any non-covalent complex formation between Q β and C₆₀. Thus, the lower mobility band indicates successful covalent conjugation. Quantification of C₆₀ moieties per Q β particle was determined based on density analysis and ImageJ band analysis tool (<http://imagej.nih.gov/ij>). It was estimated that 60±10% C₆₀ drugs were attached to Q β (Fig. S1). Non-specific binding of C₆₀ to Q β was not observed; this was tested by mixing Q β and C₆₀, while omitting the coupling reagents, followed by analysis on native and denaturing gels.

Fluorescently-labeled Q β -C₆₀ formulations were evaluated in tissue culture using human prostate cancer cells. Since invasive surgery at the prostate can be associated with various

complications and chemotherapy induces many adverse effects, PDT is a desired alternative for the treatment of prostate cancer. We chose PC-3 cells, a highly metastatic cell line, because it is a well-characterized model for prostate cancer, and we have already developed methods to target and image PC-3 derived tumor xenografts in animal models.¹¹ First cell interactions were evaluated using confocal microscopy to assess whether conjugation of C₆₀ affected cellular uptake. Live PC-3 cells were incubated with 5 μg of Qβ-O488 and Qβ-O488-C₆₀ at 37°C, 5% CO₂ for 3 h. Post incubation, cells were washed thoroughly, fixed, cell membranes were stained using wheat germ agglutinin (WGA) conjugated with Alexa Fluor 555 (WGA-A555) (Invitrogen), and cell nuclei were stained using 4',6-diamidino-2-phenylindole (DAPI) (MP Biomedicals). Confocal images were obtained using Olympus FluoView™ FV1000 LSCM and data processed using ImageJ software. We had previously shown that Qβ and Qβ-C₆₀ complexes are taken up by breast cancer cells,¹⁴ and we show here that the VNP delivery vehicle is also taken up by prostate cancer cells (Fig. 2A). Instead of being widely distributed throughout the cytoplasm, the punctate pattern indicates uptake via endocytosis and targeting to the endolysosomal compartment; the cell interaction is consistent with data reported in the literature.^{12e,15} Further, uptake is inhibited at 4°C thus further supporting internalization through an energy-dependent endocytosis mechanism. Our data indicate that the display of multiple copies of hydrophobic C₆₀ drugs does not inhibit prostate cancer cell uptake.

Next, drug efficacy was tested using white light therapy. Triplicates of Qβ, C₆₀, and Qβ-C₆₀ in 100 μL of medium were added to live cells in increasing amounts, matching the concentrations of Qβ and C₆₀ to Qβ-C₆₀, respectively. Following incubation for 3 h, the medium was removed, the cells were washed with saline, and 100 μL of fresh medium was added. The cells were returned to the incubator for 24 h to allow bound particles to be internalized. A mirror was then used to reflect white light from a Proxima DP1000x projector onto the cells in a 6 by 8 in. rectangle at a dose of 2 mW/cm² (Fig. 2B). The cells were irradiated for 1 h (6.4 J/cm²). The cell plate was then incubated at 37°C for 96 h. Cell viability was measured using an XTT cell proliferation assay kit (ATCC). Cell viability data are shown in Fig. 2C. Toxicity of Qβ was not apparent in the dark, indicating that the biological nanomaterial is not cytotoxic, even at high concentrations (0.42 μM, i.e. 1.67×10⁹ particles/cell). Data indicate increased photodynamic activity of the Qβ-C₆₀ versus free drug compound when used at 25 μM drug concentration. Up to 70% of PC-3 cells treated with the Qβ-C₆₀ formulation were killed using white light therapy, while only 50% of cells treated with propargyl-O-PEG-C₆₀ alone were found dead (p < 0.05), thus indicating an advantage of delivering C₆₀ drugs to cancer cells using VNPs.

Besides the increased photodynamic activity of VNP-C₆₀ compared to free drug, the nanoparticle carrier offers further advantages, i.e. multivalent formulations can be designed. Qβ-C₆₀ displays 60 C₆₀ moieties, i.e. 660 reactive Lys side chains remain available for further functionalization with, for example, targeting ligands such as the peptide bombesin,¹¹ and chemotherapies.^{12e} The synergistic effect from the multivalent display of targeting ligands, along with the increased activity seen here from drug delivery via a carrier suggest the development of targeted combination therapies has the potential to greatly enhance the effectiveness of PDT. Furthermore, it should be noted that propargyl-PEG-C₆₀ had low solubility in buffered solutions (precipitation was noted at 100 μM concentration in 20% DMSO/buffer mixtures). By visual inspection, the 25 μM concentration used for the *in vitro* studies was the highest concentration without noticeable precipitation. Conjugation to Qβ increased the solubility such that there was no precipitation at a concentration of 4.2 mg/mL Qβ-C₆₀, which corresponds to an concentration of 100 μM C₆₀.

Conclusions

We have successfully demonstrated conjugation of C₆₀ to Q β using click chemistry as a highly efficient method for the development of biocompatible therapeutic agents for PDT. We have shown that using Q β as a scaffold enhances cellular internalization of the C₆₀ by prostate cancer cells, resulting in greater therapeutic efficacy. In addition, we found that the propargyl-O-PEG-C₆₀ derivative alone in the absence of light therapy also did not result in cell toxicity. However, its insolubility in water detracts from its potential as a PDT drug by itself. Overall, Q β -C₆₀ is a promising platform for PDT, with additional sites for functionalization with additional biomedically relevant moieties, such as targeting ligands or additional drugs. Future work will explore *in vivo* applications of Q β -C₆₀ for targeted and combination therapies.

Supplementary Material

Refer to Web version on PubMed Central for supplementary material.

Acknowledgments

This work was supported by NIH/NIBIB grants R00 EB009105 and P30 EB011317 (NFS); T32 EB007509 training fellowship (AMW), U. Dayton Honors Thesis Research Fellowship (MJR); Alcoa undergraduate student funding (ACY). We thank Prof. Comfort (U. Dayton) for co-mentorship to MJR and Prof. Finn and Dr. Preslovski (TSRI) for providing Q β plasmids and THTPA ligand.

References

1. Moore CM, Pendse D, Emberton M. *Nat Clin Pract Urol*. 2009; 6:18. [PubMed: 19132003]
2. (a) Wolun-Cholewa M, Piedad B. *Ginekol Pol*. 2011; 82:503. [PubMed: 21913427] (b) Evans CL, Abu-Yousif AO, Park YJ, Klein OJ, Celli JP, Rizvi I, Zheng X, Hasan T. *PLoS One*. 2011; 6:e23434. [PubMed: 21876751] (c) Smith GS, Therrien B. *Dalton Trans*. 2011; 40:10793. [PubMed: 21858344] (d) Zhu X, Lu W, Zhang Y, Reed A, Newton B, Fan Z, Yu H, Ray PC, Gao R. *Chem Commun (Camb)*. 2011; 47:10311. [PubMed: 21853198]
3. (a) Zhao B, Yin JJ, Bilski PJ, Chignell CF, Roberts JE, He YY. *Toxicol Appl Pharmacol*. 2009; 241:163. [PubMed: 19695274] (b) Samia AC, Chen X, Burda C. *J Am Chem Soc*. 2003; 125:15736. [PubMed: 14677951] (c) Anderson CY, Freye K, Tubesing KA, Li YS, Kenney ME, Mukhtar H, Elmets CA. *Photochem Photobiol*. 1998; 67:332. [PubMed: 9523532] (d) Cheng Y, Meyers JD, Broome AM, Kenney ME, Basilion JP, Burda C. *J Am Chem Soc*. 2011; 133:2583. [PubMed: 21294543]
4. Bakry R, Vallant RM, Najamul-Haq M, Rainer M, Szabo Z, Huck CW, Bonn GK. *Int J Nanomedicine*. 2007; 2:639. [PubMed: 18203430]
5. (a) Arbogast JW, Darmanyan AP, Foote CS, Rubin Y, Diedricj FN, Alvarez MM, Anz SJ, Whetten RL. *J Phys Chem*. 1991; 95:11. (b) Nakanishi I, Ohkubo K, Fujita S, Fukuzumi S, Konishi T, Fujitsuka M, Ito O, Miyata N. *J Chem Soc, Perkin Trans 2*. 2002; 2:1829.
6. Kovoichich M, Espinasse B, Auffan M, Hotze EM, Wessel L, Xia T, Nel AE, Wiesner MR. *Environ Sci Technol*. 2009; 43:6378. [PubMed: 19746740]
7. (a) Hu Z, Zhang C, Huang Y, Sun S, Guan W, Yao Y. *Chem Biol Interact*. 2012; 195:86. [PubMed: 22108244] (b) Liao F, Saitoh Y, Miwa N. *Oncol Res*. 2011; 19:203. [PubMed: 21542456] (c) Metanawin T, Tang T, Chen R, Vernon D, Wang X. *Nanotechnology*. 2011; 22:235604. [PubMed: 21483045] (d) Otake E, Sakuma S, Torii K, Maeda A, Ohi H, Yano S, Morita A. *Photochem Photobiol*. 2010; 86:1356. [PubMed: 20796243] (e) Lee I, Mackeyev Y, Cho M, Li D, Kim JH, Wilson LJ, Alvarez PJ. *Environ Sci Technol*. 2009; 43:6604. [PubMed: 19764224] (f) Akiyama M, Ikeda A, Shintani T, Doi Y, Kikuchi J, Ogawa T, Yogo K, Takeya T, Yamamoto N. *Org Biomol Chem*. 2008; 6:1015. [PubMed: 18327326] (g) Ikeda A, Doi Y, Nishiguchi K, Kitamura K, Hashizume M, Kikuchi J, Yogo K, Ogawa T, Takeya T. *Org Biomol Chem*. 2007; 5:1158.

- [PubMed: 17406710] (h) Iwamoto Y, Yamakoshi Y. *Chem Commun (Camb)*. 2006;4805. [PubMed: 17345735]
8. Suci PA, Varpness Z, Gillitzer E, Douglas T, Young M. *Langmuir*. 2007; 23:12280. [PubMed: 17949022]
9. (a) Stephanopoulos N, Tong GJ, Hsiao SC, Francis MB. *ACS Nano*. 2010; 4:6014. [PubMed: 20863095] (b) Tong GJ, Hsiao SC, Carrico ZM, Francis MB. *Journal of the American Chemical Society*. 2009; 131:11174. [PubMed: 19603808]
10. Pokorski JK, Steinmetz NF. *Mol Pharm*. 2011; 8:29. [PubMed: 21047140]
11. Steinmetz NF, Ablack AL, Hickey JL, Ablack J, Manocha B, Mymryk JS, Luyt LG, Lewis JD. *Small*. 2011; 7:1664. [PubMed: 21520408]
12. (a) Ashley CE, Carnes EC, Phillips GK, Durfee PN, Buley MD, Lino CA, Padilla DP, Phillips B, Carter MB, Willman CL, Brinker CJ, Caldeira J, do C, Chackerian B, Wharton W, Peabody DS. *ACS Nano*. 2011; 5:5729. [PubMed: 21615170] (b) Wu W, Hsiao SC, Carrico ZM, Francis MB. *Angew Chem Int Ed Engl*. 2009; 48:9493. [PubMed: 19921725] (c) Lockney DM, Guenther RN, Loo L, Overton W, Antonelli R, Clark J, Hu M, Luft C, Lommel SA, Franzen S. *Bioconjug Chem*. 2011; 22:67. [PubMed: 21126069] (d) Zhao Q, Chen W, Chen Y, Zhang L, Zhang J, Zhang Z. *Bioconjug Chem*. 2011; 22:346. [PubMed: 21338097] (e) Pokorski JK, Breitenkamp K, Liepold LO, Qazi S, Finn MG. *J Am Chem Soc*. 2011; 133:9242. [PubMed: 21627118]
13. (a) Stephanopoulos N, Tong GJ, Hsiao SC, Francis MB. *ACS Nano*. 2010; 4:6014. [PubMed: 20863095] (b) Suci PA, Varpness Z, Gillitzer E, Douglas T, Young M. *Langmuir*. 2007; 23:12280. [PubMed: 17949022]
14. Steinmetz NF, Hong V, Spoerke ED, Lu P, Breitenkamp K, Finn MG, Manchester M. *J Am Chem Soc*. 2009; 131:17093. [PubMed: 19904938]
15. Pokorski JK, Hovlid ML, Finn MG. *Chembiochem*. 2011; 12:2441. [PubMed: 21956837]

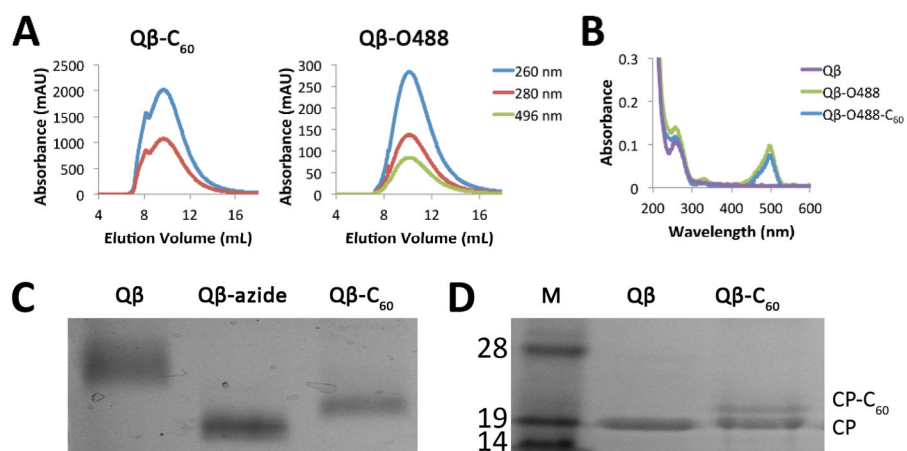


Fig. 1. (A) SEC of Q β -C₆₀ and Q β -O488. Intact particles elute at approximately 10 mL. The co-elution of O488 (496 nm) validates attachment. (B) UV/visible spectra of Q β , Q β -O488, and Q β -O488-C₆₀. (C) Native agarose gel. (D) Q β and Q β -C₆₀ proteins separated on a denaturing 4–12% SDS-PAGE. M=SeeBlue Plus2 molecular weight marker. Approximately 33% of the Q β coat proteins (CPs) are labeled with C₆₀ as estimated by densitometric analysis using ImageJ software.

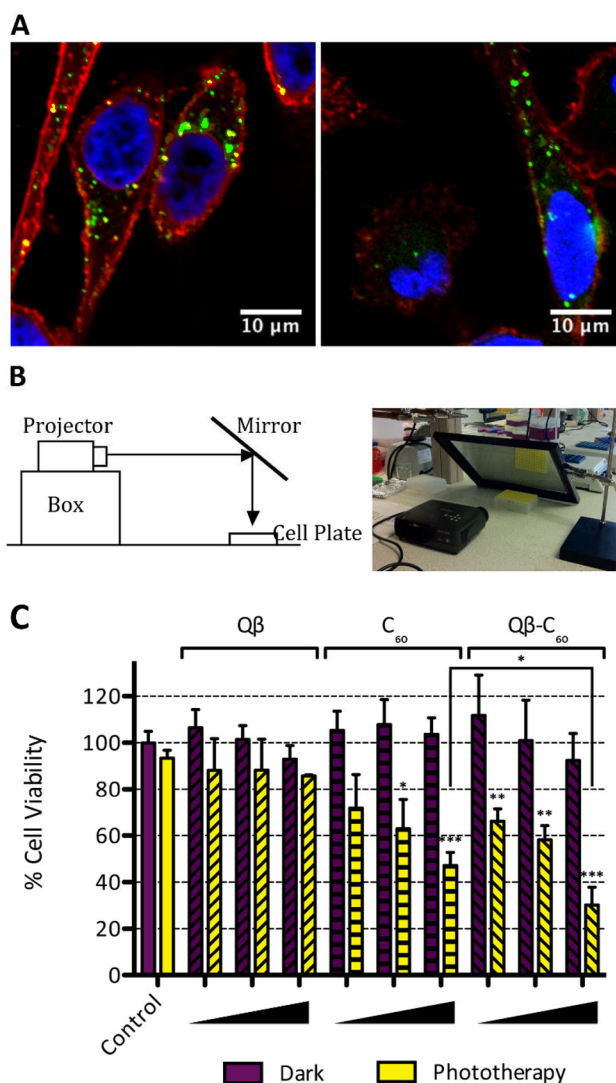
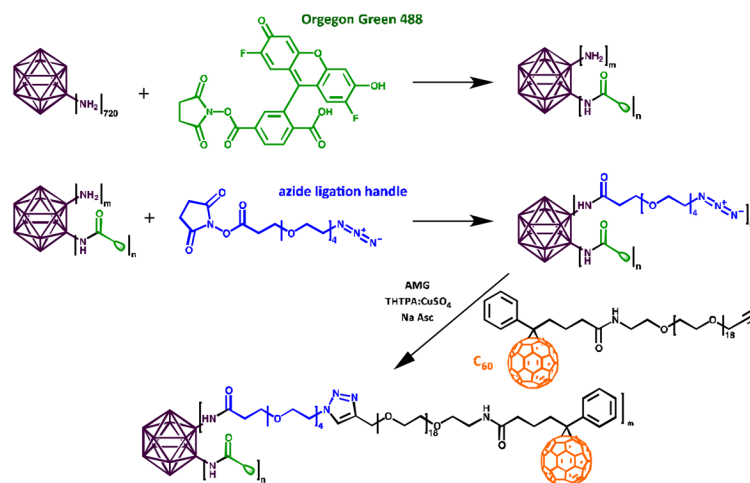


Fig. 2. (A) Confocal microscopy of PC-3 cells treated with Q β -O488 (left) and Q β -O488-C₆₀ (right) show internalization (green). The nucleus was stained with DAPI (blue), and the cell membrane was stained with Alexa Fluor 555-labeled wheat germ agglutinin (red). (B) Experimental set-up for white light PDT. (C) Cell viability assay indicates cell killing after an hour of phototherapy. Three concentrations were tested: 1, 10, and 25 μ M C₆₀ (corresponding to 0.0167, 0.1667, and 0.4167 μ M Q β). Statistical comparisons were made to the dark control and significance is indicated by asterisks (* p<0.05, ** p<0.01, *** p<0.001). There was a significant difference between the levels of cell killing of Q β -C₆₀ compared to free C₆₀ at 25 μ M drug concentration (p<0.05).



Scheme 1.
Bioconjugation of O488 and C₆₀ to Q β .